FULL PAPER

Doxorubicin-Loaded Single Wall Nanotube Thermo-Sensitive Hydrogel for Gastric Cancer Chemo-Photothermal Therapy

Minyu Zhou, Shuhan Liu, Yaqi Jiang, Huanrong Ma, Min Shi, Quanshi Wang, Wen Zhong, Wangjun Liao, and Malcolm M. Q. Xing**

Single wall carbon nanotube (SWNT) based thermo-sensitive hydrogel (SWNT-GEL) is reported, which provides an injectable drug delivery system as well as a medium for photothermal transduction. SWNT-hydrogel alone appears to be nontoxic on gastric cancer cells (BGC-823 cell line) but leads to cell death with NIR radiation through a hyperthermia proapoptosis mechanism. By incorporating hyperthermia therapy and controlled in situ doxorubicin (DOX) release, DOX-loaded SWNT-hydrogel with NIR radiation proves higher tumor suppression rate on mice xenograft gastric tumor models compared to free DOX without detectable organ toxicity. The developed system demonstrates improved efficacy of chemotherapeutic drugs which overcomes systemic adverse reactions and presents immense potential for gastric cancer treatment.

1. Introduction

Gastric cancer (GC), a second leading mortality of cancer, represents one of the most common malignancies worldwide. Though systemic chemo agents and surgical excision are preferred approach in the early-stage gastric cancer treatment, drug resistance and unresectable lumps require more advanced therapeutic strategy.[1] Chemotherapeutics exert extensive adverse reactions when systemically injected. For example, approximately 10% of patients treated with doxorubicin (DOX) will take the risk of cardiotoxicity or develop cardiac complications.[2] Besides, tumor diversity evades the efficacy of monotherapy, not to mention the exiguity of molecular targeted agents toward gastric cancer also limits its treatment. Currently, the only approved targeted drug for primary GC in clinical application is trastuzumab, which requires patients' HER-2 expression when applied as target drugs.[3] Trastuzumab is known as one kind of targeted monoclonal antibody agents, although better tolerated and less toxicity was obtained than conventional anticancer drugs, monoclonal antibodies may cause infusion-related reactions like other infusional agents, and recently there are reports on severe delayed hypersensitivity reaction induced by trastuzumab.[4] Over the past few decades, nanomedicine with the emergence of new nanoparticles has obtained extensive attentions for they can function as cancer diagnose agents, drug delivery and release system, etc.[5] However, the low efficiency of nanoparticles' homing to tumor location through intravenous injection is one of the challenges demanding prompt solution.

Near-infrared (NIR) radiation has drawn intense attentions as an efficient stimulus in photo-dynamic therapy. There are two justifiable superiorities to apply NIR light to tumor therapy: primarily, the absorbing window of NIR, ≈650–1000 nm, by skin and tissue with minimum absorption compared with other radiations such as 10 nm to 5 pm for X-ray;[6] furthermore, NIR can infiltrate tissue from micrometers to centimeters, which set the stage for human body applications.[7]

Some nanomaterials, such as carbon nanotubes (CNTs), can absorb NIR and produce local high temperature to kill cancer cells. Single wall carbon nanotube (SWNT), which belongs to one category of CNTs and has been employed in nanomedicine

Dr. M. Zhou, S. Liu, Dr. Y. Jiang, Dr. H. Ma, Dr. M. Shi, Prof. W. Liao, Prof. M. M. Q. Xing
Department of Oncology
Nanfang Hospital
Southern Medical University
Guangzhou Avenue North 1838
Guangzhou 510515, China
E-mail: nfyyliaowj@163.com; malcolm.xing@umanitoba.ca
S. Liu, Prof. M. M. Q. Xing
Department of Mechanical Engineering
Department of Biochemistry and Medical Genetics
University of Manitoba
Winnipeg MB R3T 5V6, Canada
Dr. Q. Wang
Nanfang PET Center
Nanfang Hospital
Southern Medical University
Guangzhou, China
Prof. W. Zhong
Department of Biosystem Engineering
University of Manitoba
Winnipeg, Canada
Prof. M. M. Q. Xing
Children's Hospital Research Institute of Manitoba
Winnipeg, Canada
Prof. M. M. Q. Xing
Department of Mechanical Engineering
75A Chancellors Circle
University of Manitoba
Winnipeg MB R3T 5V6, Canada

DOI: 10.1002/adfm.201501434

© 2015 WILEY-VCH Verlag GmbH & Co. KGaA, Weinheim

for several years, is also an ideal drug carrier in the application of cancer treatment because of their large surface area and unique physical properties (optical and electrical property).[8] Therefore, CNTs could be used in the diagnosis and treatment toward tumors, especially those deeply growing inside human body,[8b] such as hysteroma, which is hard to detect and cure in an early stage by traditional methods.[9] In addition, the chemotherapy drugs and some biomolecules could be noncovalently or covalently coated into CNTs.[10] These traits of CNTs provide a compelling evidence of their application in nanomedicine.

Poly(*n*-isopropyl acrylamide) (pNIPAM) thermo-sensitive polymer has been widely used to detach cells from culture dish without enzyme catalyzing and is nontoxic. It is based on a critical solution temperature of 33 °C, above which pNIPAM experiences a solution(sol) to gelation(gel) transition; thus, hydrogels form at body temperature.[11] As a drug carrier, pH-sensitive pNIPAM microgel can carry chemotherapeutic agent to kill cancer cells efficiently in vitro.[12] Heretofore, it has been widely studied on using pNIPAM gel or CNTs alone for different drug delivery or cancer therapy, while no report was seen on integrating both pNIPAM and CNTs together to treat GC from in vitro to in vivo.

To this end, we reported single wall carbon nanotube based injectable thermo-sensitive hydrogel (SWNT-GEL) to deliver DOX in xenograft GC mice treatment. First, injectable hydrogel can directly deliver DOX to the tumor site allowing it contributing anticancer effect in situ; meanwhile, NIR can provide hyperthermia therapy by penetrating tissues to stimulate SWNT located in tumor site, which finally attains chemo-combined photothermal therapy (**Scheme 1**).

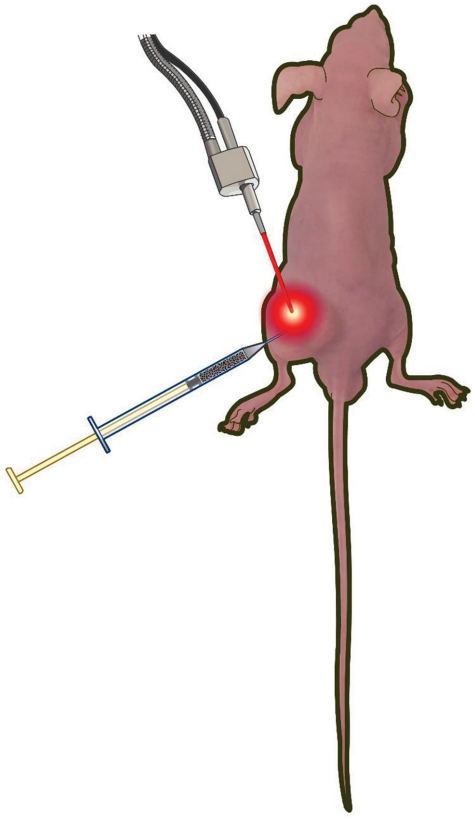

Scheme 1. Xenograft tumor model is established by subcutaneous injection of BGC-823 gastric cancer cells. DOX/SWNT-GEL is administrated intratumorly and then the mouse receives NIR laser irradiation at the tumor site.

2. Results

2.1. Basic Characterization of DOX/SWNT-GEL

We first synthesized gelatin/SWNT-(3-aminopropyl) trimethoxysilane (APTS)-NH_2 and then copolymerized pNIPAM for the preparation of thermo-sensitive hydrogel (SWNT-GEL) and employed it for anti-cancer drug delivery as well as for hyperthermia therapy, following which the DOX-loaded SWNT-GEL(DOX/SWNT-GEL) was prepared. FTIR was employed for the characterization of gelatin, SWNT-APTS, gelatin/SWNT-APTS, NIPAM, PNIPAM-NH_2, and gelatin/SWNT-APTS-NH_2, respectively. As elucidated in **Figure 1**A, the band at 1104 cm^{-1} displayed in the spectrum of gelatin/SWNT-APTS was attributed to Si–O–Si resulted from SWNT-APTS. The band at 1103 cm^{-1} shown in the spectrum of gelatin/SWNT-APTS-NH_2 was attributed to Si–O–Si from gelatin/SWNT-APTS. We concluded that gelatin/SWNT-APTS-NH_2 was successfully prepared from gelatin/SWNT-APTS and pNIPAM-NH_2 as exhibited in Figure 1A.

PNIPAM is known as a thermo-sensitive polymer. When the temperature is lower than the lower critical solution temperature (33 °C), the H-bond between N, O atoms from amid bonds and water molecules will be formed; when the temperature is higher than lower critical solution temperature, the H-bond will be blocked and the polymer chain will transform to a coiled structure. The SWNT could disperse in the solution of pNIPAM in low temperature because the amphiphilic polymer chain of pNIPAM could cover onto the surface of SWNT. When the temperature is higher than 33 °C, the SWNT will aggregate into little trusses due to the contraction of pNIPAM polymer's chain conformation and the hydrophobic SWNT surface will be revealed to water.

The SWNT-GEL powder was dissolved in the deionized water to reach a final concentration of 20 mg mL^{-1} (w/v); Figure 1B (left) showed the liquid state of the solution in room temperature, when temperature reached 37 °C, which was higher than lower critical solution temperature of pNIPAM, the hydrogel formed (Figure 1B, right). Furthermore, we explored the microstructures of SWNT-based hydrogel with TEM, as shown in Figure 1C, where SWNTs were imbedded in the hydrogel. Additionally, the drug release curve of DOX/SWNT-GEL was depicted during a period of 28 d. As exhibited in Figure 1D, in the first day of incubation, there was over 20% of DOX released from the drug-loading system, while in the following 10 d, the cumulative release of DOX from the gelated SWNT-hydrogel in PBS was approximately 50%. The remanent DOX was released into PBS gradually in the following days and the accumulated DOX release reached to about 96% at the 28th day of record; which illustrated a continuous drug release and delivery function of SWNT-GEL.

© 2015 WILEY-VCH Verlag GmbH & Co. KGaA, Weinheim

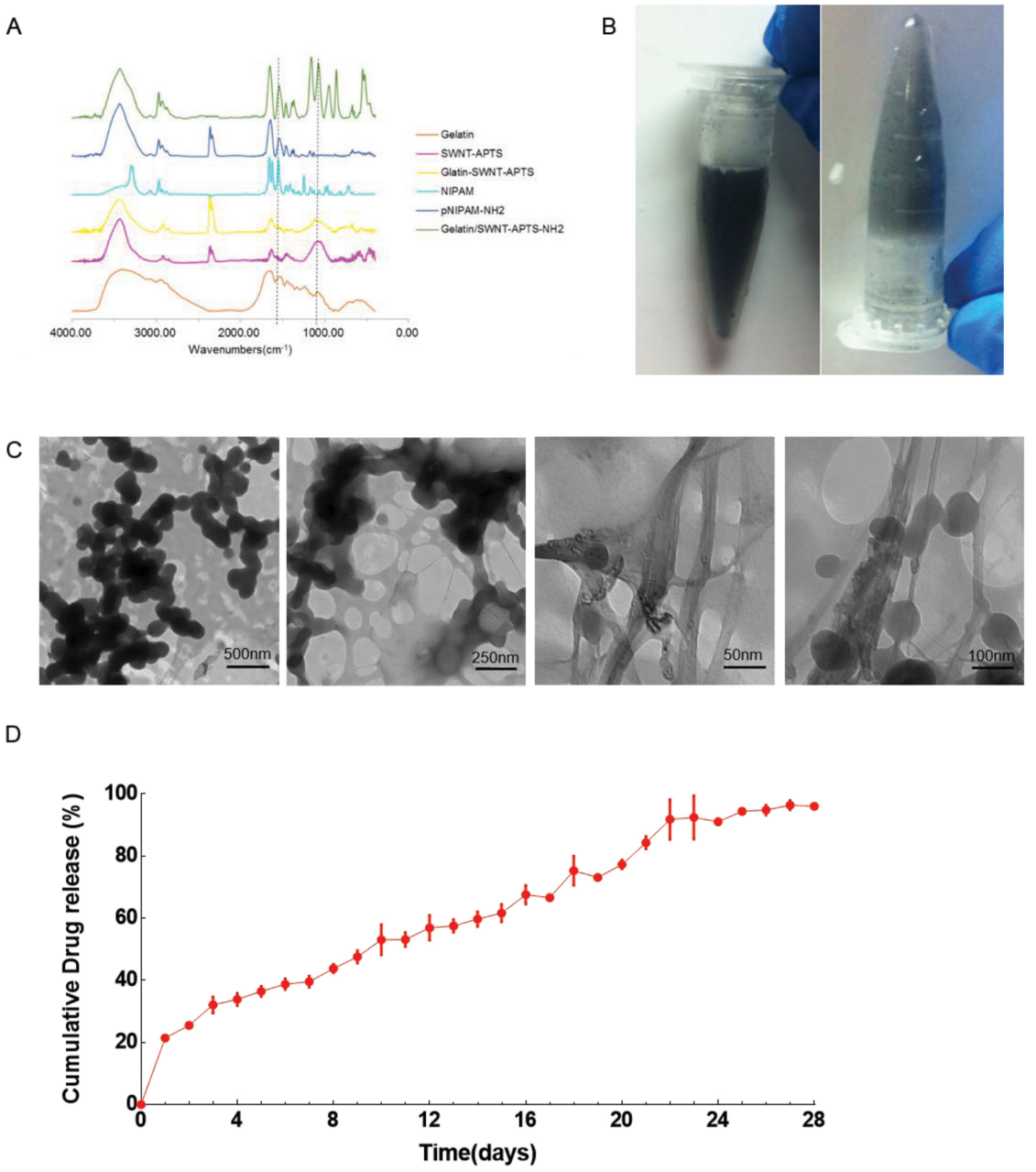

Figure 1. The basic characterization of gelatin/SWNT-APTS-NH_2. A) FT-IR comparison of gelatin, SWNT-APTS, gelatin/SWNT-APTS, NIPAM, pNIPAM-NH_2 and gelatin/SWNT-APTS-NH_2. B) The gel formation for gelatin/SWNT-APTS-NH_2 hydrogel. Image in the left was taken in room temperature while image in the right was taken after 1 min heat in 37 °C water bath. C) TEM characterization of gelatin/SWNT-APTS-NH_2 hydrogel. D) DOX release profile from SWNT-GEL in PBS for 28 d at a constant temperature of 43 °C, the data was calculated for cumulative drug release for 28 d and shown as mean ± SD of three independent experiments.

2.2. In Vitro Cellular Uptake of DOX/SWNT-GEL

To testify whether the DOX/SWNT-GEL hybrid was capable to deliver DOX to cancer cells, we next carried out the in vitro cellular uptake assay. The gastric cancer cell line BGC-823 cells were incubated in culture medium added with DOX/SWNT-GEL (DOX concentration: 2 μg mL^{-1}), and cellular uptake status was evaluated by red fluorescence intensity under fluorescence microscope at predetermined time intervals, which indicated the density of DOX accumulated in cancer cells. As shown in **Figure 2**, the red fluorescence of DOX increased as incubation time prolonged (from 0.5 to 24 h); meanwhile, most of the red fluorescence overlaps with the blue fluorescence (which indicated nucleus), demonstrating DOX entering into cancer cell nucleus, where DOX exert its anti-cancer effect.

© 2015 WILEY-VCH Verlag GmbH & Co. KGaA, Weinheim

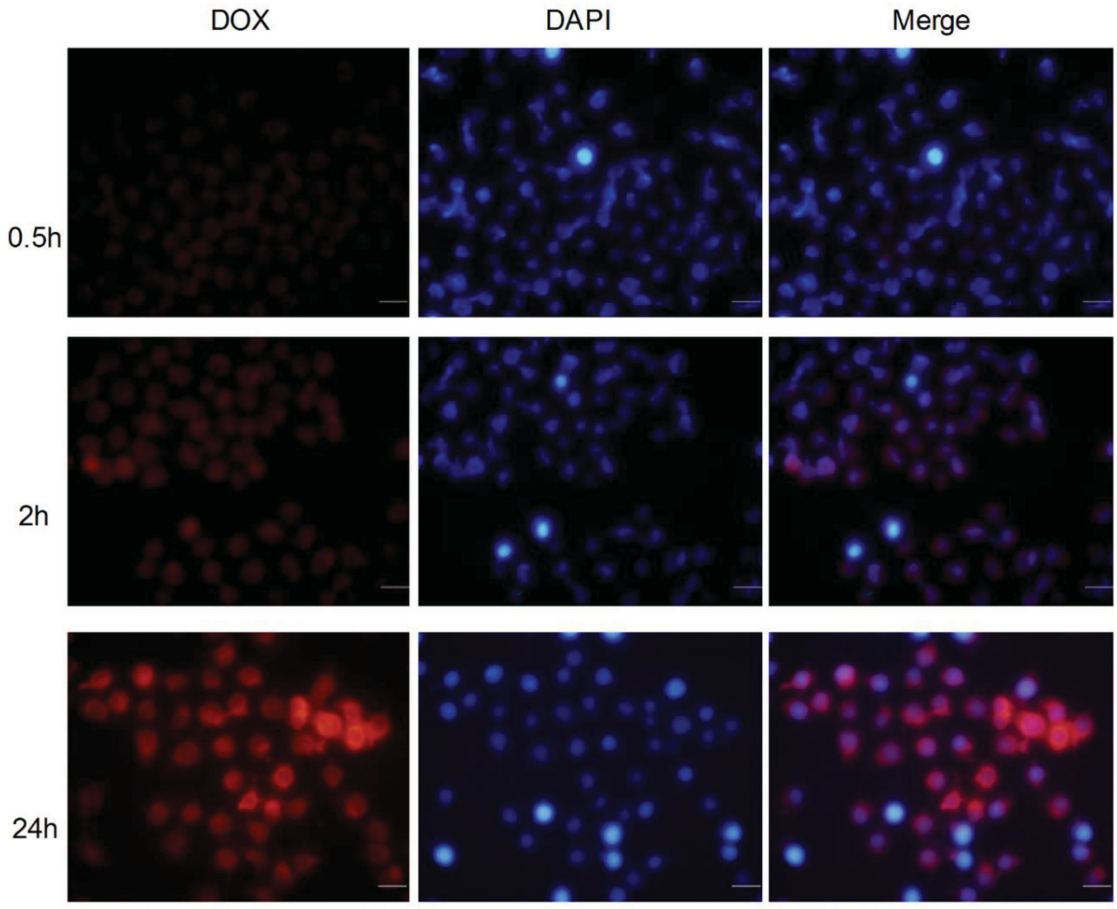

Figure 2. In vitro cellular uptake rate of DOX/SWNT-GEL. BGC-823 cells were incubated with DOX/SWNT-GEL hybrid for appointed time intervals (0.5, 2, and 24 h) and its cellular uptake was examined by fluorescent microscope. Scale bar: 100 μm.

2.3. DOX/SWNT-GEL Affects Cell Viability through a Pro-Apoptosis Mechanism

To assess the cytotoxicity of free DOX and NIR-irradiated SWNT-GEL on BGC-823 cells, cell viability was determined. Cells were incubated with free DOX or SWNT-GEL at different concentrations for 24 h; additionally, the SWNT-GEL-treated groups received NIR light radiation for different time periods (0 s, 15 s, and 3 min). Free DOX showed a dose-dependent cytotoxicity on BGC cells with an IC_{50} value of ≈3μg mL^{-1} (**Figure 3**A). While SWNT-GEL without irradiation did not show any toxicity to BGC cells at the tested concentrations, the NIR-irradiated SWNT-GEL caused a reduction in cell viability with both exposure time prolonged and concentration of the nanomaterial increased (Figure 3B), which illustrated the nanoparticle alone did not affect cell growth while due to the hyperthermia effect induced by NIR-irradiated SWNT, cell viability was reduced up to 30% compared with no NIR treatment group. The control group (with the SWNT-GEL concentration 0 μg mL^{-1}) had nearly no cell viability change even after NIR irradiation, which indicated the energy produced by NIR irradiation did not damage cancer cells.

To evaluate whether DOX/SWNT-GEL following laser treatment has better apoptotic effect on cancer cells than free DOX, the flow cytometry assay was conducted to evaluate cell apoptosis rate. Annexin V FITC and propidium iodide (PI) were used as label of apoptosis cells. As shown in Figure 3C, cell debris was distributed in four different quadrants (upper panel), right upper quadrant and right lower quadrant represented the amount of early and late apoptotic cells, respectively, which were both included in the calculation of apoptosis. The BGC cells pretreated with DOX/SWNT-GEL incorporated by NIR irradiation presented a higher apoptosis rate than free DOX-treated groups (lower panel); as contrast, the PBS control group obtained most intact cells and least apoptotic cells, which suggests NIR irradiated SWNT had a pro-apoptotic effect through a hyperthermia-dependent mechanism.

2.4. Inhibition of Tumor Growth In Vivo by DOX/SWNT-GEL

To investigate the suppression effect of DOX/SWNT-GEL on tumor growth, xenograft gastric cancer tumor model was established with Balb/c nude mice. When the tumor volume reached about 100 mm^3, a total of 24 mice were randomly assigned to four groups and intratumorly injected with PBS, free DOX, SWNT-GEL, and DOX/SWNT-GEL, respectively. Half of mice in each group were taken for NIR irradiation

© 2015 WILEY-VCH Verlag GmbH & Co. KGaA, Weinheim

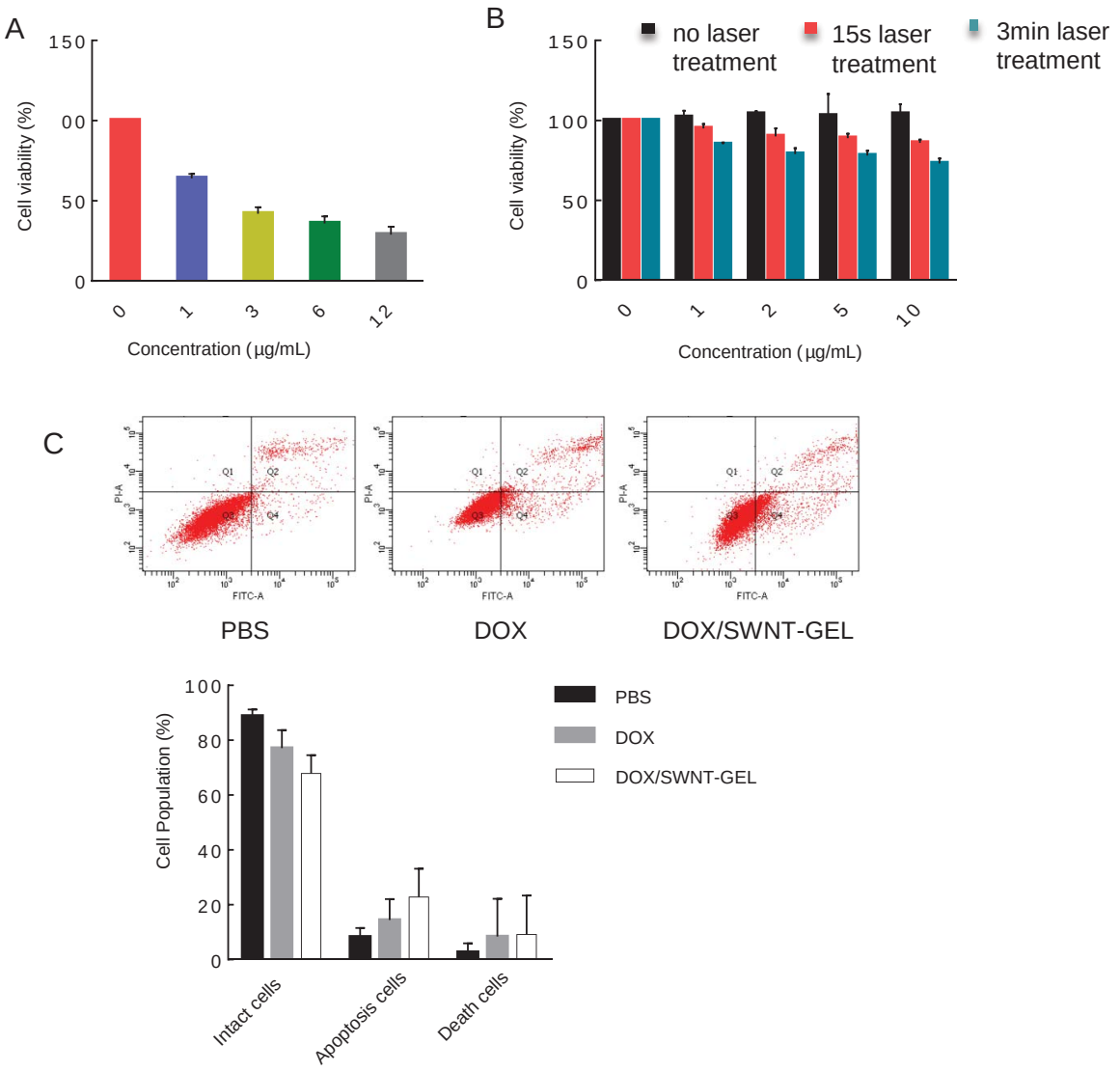

Figure 3. In vitro cytotoxicity assays. A) MTT assay of doxorubicin on BGC-823 cell. B) MTT assay of gelatin/SWNT-APTS-NH_2 hydrogel on BGC-823 cell. C) Flow cytometry results of the apoptotic effects of DOX/SWNT-GEL on BGC-823 cell. The data are presented as mean ± SD from three independent experiments.

at the tumor site at a power of 200 mW cm^{-1}, 976 nm wavelength, while the rest were treated without NIR radiation. After 4 weeks' observation, among mice treated with NIR radiation, the DOX/SWNT-GEL group showed a significant reduction in tumor size than the other three groups (p = 0.004 with PBS/NIR, 0.01 with DOX/NIR, 0.036 with GEL/NIR, respectively, **Figure 4**A). The average growth ratio of tumor volume reached 166% in free DOX group, while it shrank to 61.3% in DOX/SWNT-GEL group on the 27th day. This demonstrated a better tumor inhibitory effect in combined application of DOX and SWNT-GEL. Of mice without NIR radiation, the mean growth ratio was 282% in the PBS group versus 261% in the SWNT-GEL group, which indicated SWNT-GEL alone did not produce any suppression effect on tumor proliferation (Figure 4B). With respect to the DOX/SWNT-GEL group, the growth ratio in mice with NIR radiation (61.3%) was about half of those without NIR radiation (126%), disclosing a nonnegligible role of the hyperthermia effect by excited SWNT particles. To deliberate on the PBS control group alone, NIR treated mice did not show significant reduction in tumor volume compared to none-NIR treatment mice (with a p value > 0.05); on the contrary, in SWNT-GEL group alone, NIR-treated mice presented significant tumor suppression rate compared to none-NIR treatment mice, with a tumor growth ratio of 156% (with NIR) versus 261% (without NIR) on the 27th day after treatment (p value < 0.05), which concomitantly confirmed an extra tumor inhibition effect of NIR-radiated SWNT through hyperthermia conduction, and further proved NIR radiation we used was not able to induce tumor death. In brief, the combination of DOX and NIR-irradiated SWNT-based hydrogel proved the strongest tumor suppression rate, but SWNT-GEL without NIR radiation did not produce any inhibition effect.

© 2015 WILEY-VCH Verlag GmbH & Co. KGaA, Weinheim

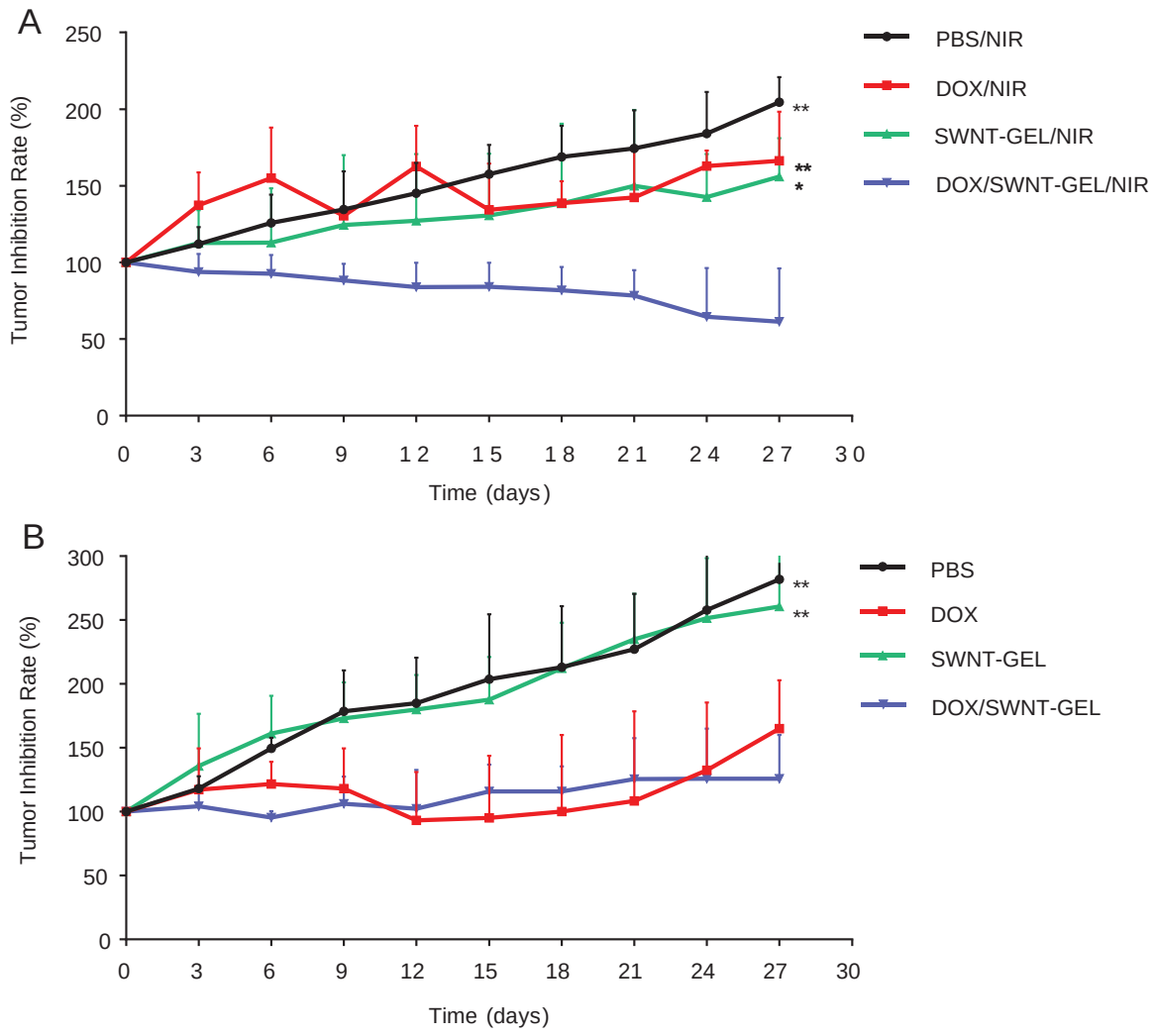

Figure 4. In vivo tumor growth rate with different treatments. A) Tumor growth rate of mice with different treatments and NIR radiation; B) tumor growth rate of mice with different treatments without NIR radiation. Data was presented as mean ± SD (*$p < 0.05$, ** $p \leq 0.01$ compared with DOX/SWNT-GEL/NIR or DOX/SWNT-GEL group).

2.5. Microstructure Change and Drug Retention Assessment In Vivo

To further validate the tumor inhibition effect, HE staining was performed on the tumor tissue 28 d after treatments, which showed a distinct morphology change with different treatments (**Figure 5**A). Evident nucleus deformation and shrink were observed in the DOX/SWNT-GEL group compared with intact and plump tumor cell nucleus in the PBS group. And nucleuses in both free DOX and SWNT-GEL groups were partially dwindled with an irregular morphologic change. In groups with SWNT-GEL injection, aggregated black dots were observed in the tissues (black arrow), which represented the SWNT particles.

To determine whether there is a longer retention of DOX in tumor tissues treated with DOX/SWNT-GEL, fluorescent microscopic evaluation was performed on tumor tissues collected 28 d after treatment. It showed a much more retention of DOX in DOX/SWNT-GEL group than in the free DOX group (Figure 5B). This suggested the in situ gel formation led to a longer duration of the drug retention in tumor site than a single injection of DOX, which may be resulted from π-stacking or π–π conjugation between DOX and SWNT.

2.6. Micro PET-CT Confirmation of Tumor Inhibition Status by DOX/SWNT-GEL

As for tumor imaging, ^{18}F-FDG tracked PET/CT scan is a frequently used technology in the detection of primary and metastasis tumors in cancer patients. It is a decent way to determine tumor biological metabolism activity through the uptake of the radiotracer ^{18}F-FDG.[13] ^{18}F-FDG is a noninvasive radioactive tracer commonly applied in the imaging and detection of tumor biological and glucose metabolism activity, which is revealed by ^{18}F-FDG uptake ability. The intensity of PET imaging represents the glucose metabolism activity of the intravital body, while CT imaging is employed for displaying the anatomic structure of the whole body. The fuse images of PET and CT showed the highest FDG uptake in the

© 2015 WILEY-VCH Verlag GmbH & Co. KGaA, Weinheim

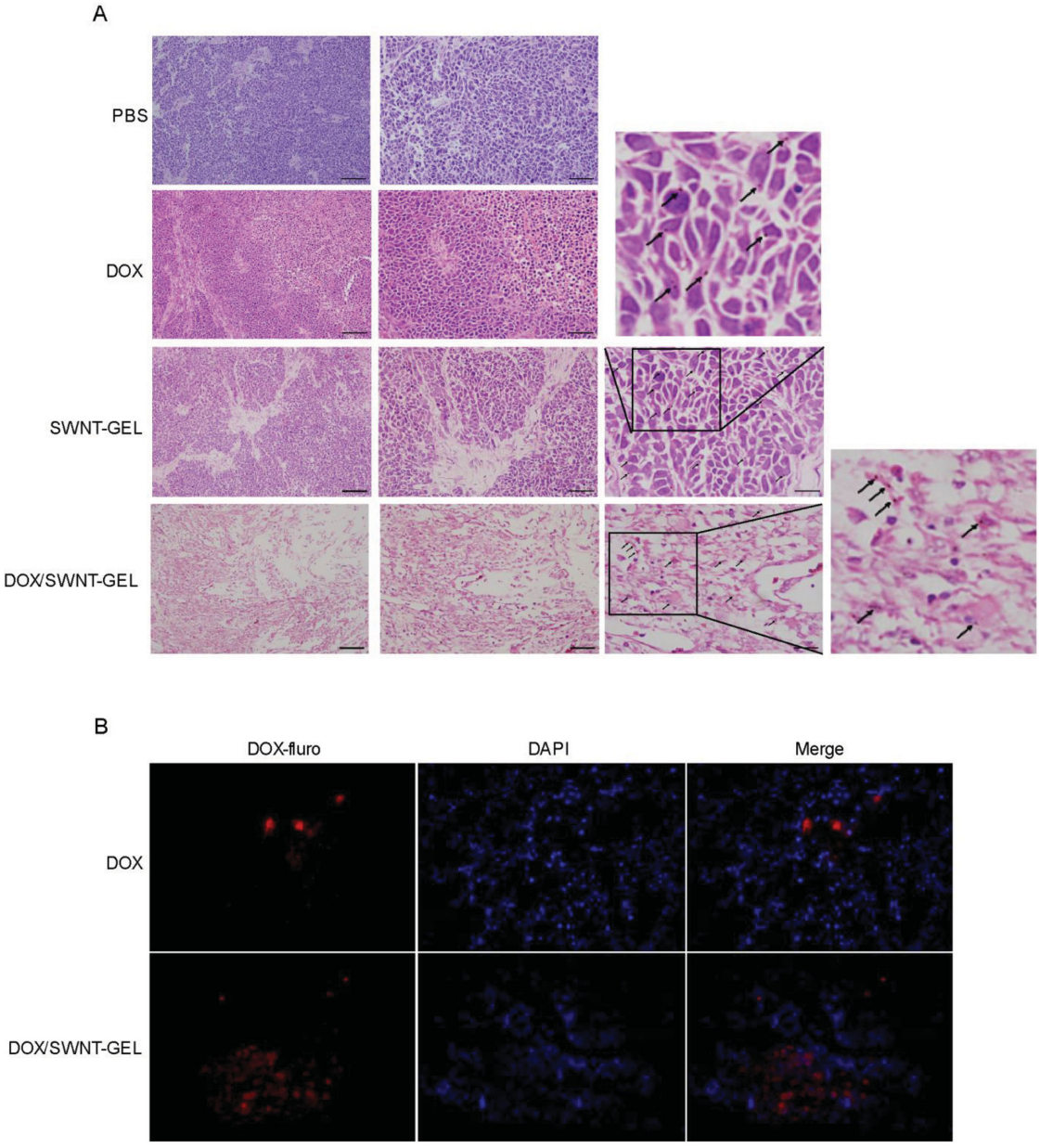

Figure 5. HE staining and fluorescence microscopic detection of tumor tissues. A) HE staining of the tumor tissue of the four groups, each panel represents one group, the black short arrows in the enlarged quadrate images (SWNT-GEL and DOX/SWNT-GEL groups, respectively, indicated by black frames and lines) point out the SWNT aggregations. Column 1: 200× magnification, column 2: 400× magnification, column 3: 1000× magnification; B) fluorescent microscopic detection of DOX retention on the 28th day after treatment, red: DOX fluorescence, blue: tumor cell nucleus stained by DAPI, merge: the location of DOX in tumor tissues. Scale bar: 100 μm.

PBS control group and the least uptake of the tracer in DOX/SWNT-GEL group (**Figure 6** and 3D movies in the Supporting Information). Generally, tumor with higher ^{18}F-FDG uptake represented a higher glucose metabolism activity and a greater likelihood of malignant biological behavior. The PET-CT scan showed concordance with the tumor volume changes and microscopic changes, mice with DOX/SWNT-GEL treatment proved a least tumor growth and lowest metabolism activity, which exhibited good anti-tumor effect of the drug-loaded SWNT-GEL.

2.7. SWNT-GEL Possess Favorable Biocompatibility without Biotoxicity

To evaluate the in vivo toxicity of the SWNT-GEL, we observed both the body weight and pathology change of organs in mice when sacrificed on the 28th day. No significant differences in the average weight of mice among groups were detected (data not shown). The microscopic assessment on the four main organs (heart, liver, kidney, spleen) indicated no obvious organ damage or tissue denaturation in mice administrated

© 2015 WILEY-VCH Verlag GmbH & Co. KGaA, Weinheim

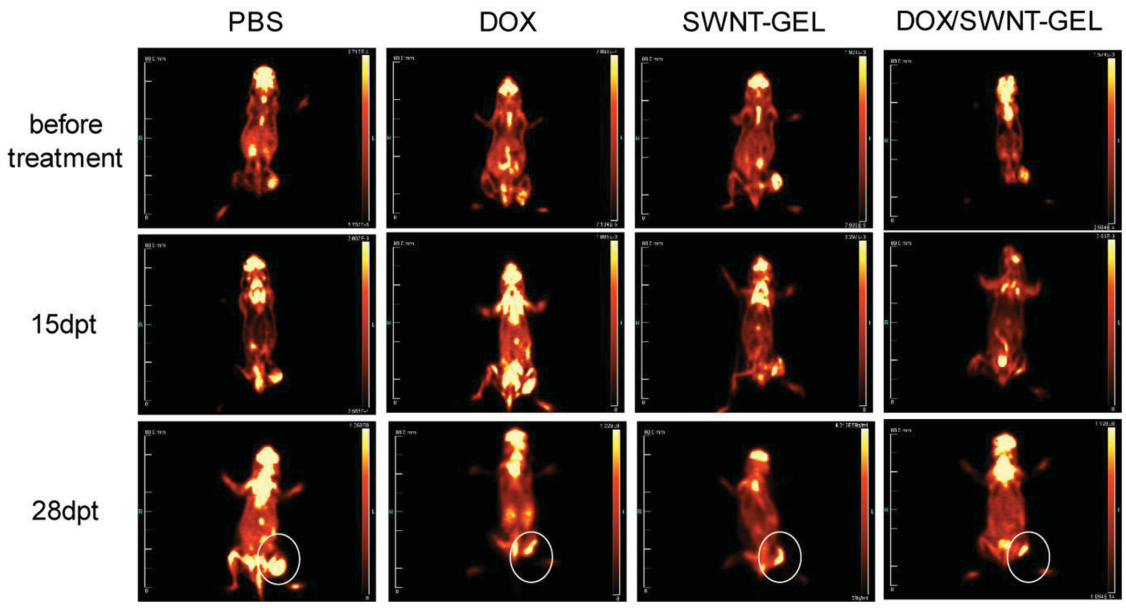

Figure 6. Micro PET-CT images of mice at different time intervals. Micro PET-CT scanning of mice before treatment, 15 d post treatment (15 dpt) and 28 d post treatment (28 dpt). The white circle indicates the position of xenograft tumor in each group.

with SWNT-GEL compared with other mice (**Figure 7**). These results manifested SWNT-GEL had no discernible toxicity on the tumor bearing mice for a period of 28 d. Although the most common adverse effect of DOX was cardiac toxicity, there was no recognizable change of heart tissue slices of the free DOX-treated group presumably due to the intratumor administration routine which reduced the systemic reaction caused by DOX.

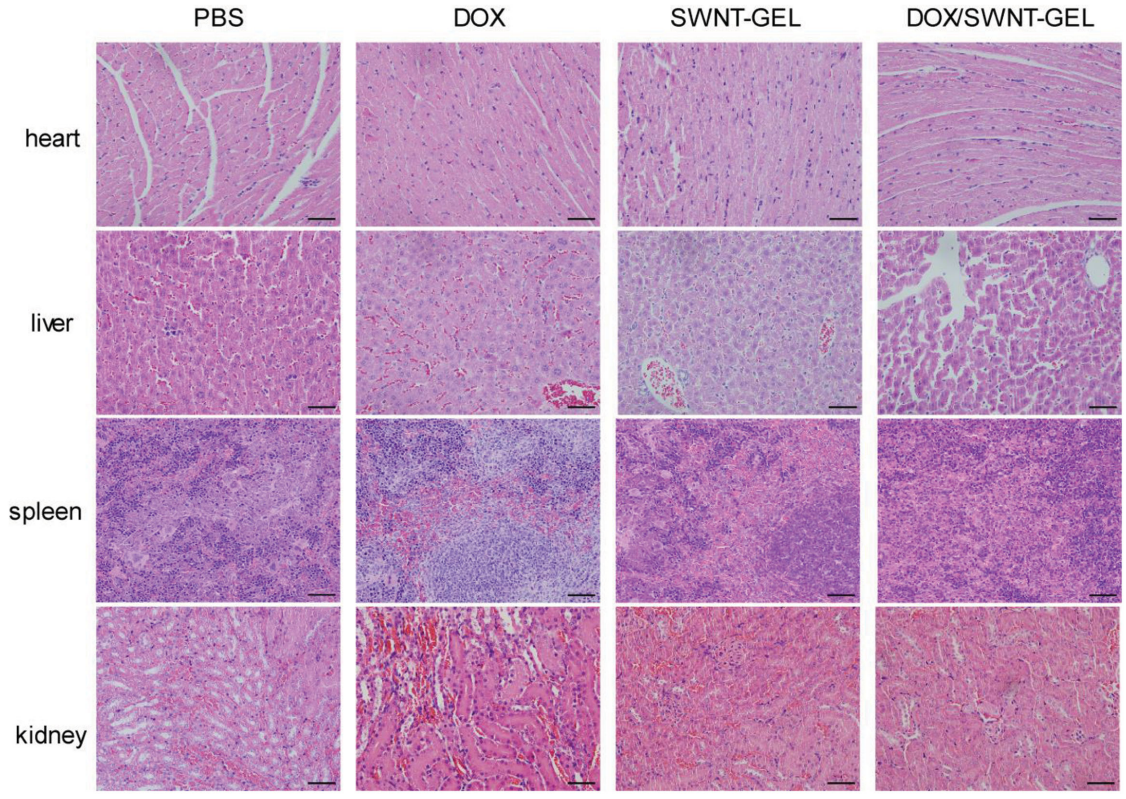

Figure 7. In vivo toxicity detection of gelatin/SWNT-APTS-NH_2 hydrogel. HE staining of heart, liver, spleen, kidney of mice in four groups, respectively. Scale bar: 100 μm.

© 2015 WILEY-VCH Verlag GmbH & Co. KGaA, Weinheim

3. Conclusion

In conclusion, we reported a DOX-loaded SWNT-GEL for gastric cancer therapy both in vitro and in vivo using NIR hyperthermia treatment. We elucidated the in vitro pro-apoptotic and the in vivo tumor inhibitory efficiency of DOX/SWNT-GEL following NIR treatment, which had exhibited better effect than free DOX treatment. Suppression of tumor growth by DOX/SWNT-GEL was further validated through micro PET-CT scanning, which showed a less ^{18}F-FDG uptake and lower tumor glucose metabolism. Organ pathology detection proved no organ toxicity and favorable biocompatibility of SWNT-GEL. Overall, our work presented in this paper demonstrated a promising prospect of SWNT-based thermo-sensitive hydrogel in the application as injectable in situ drug delivery system as well as hyperthermia therapy media.

4. Experimental Section

Materials: All chemicals were purchased from Aldrich Chemical Co. (St. Louis, MO, USA) and used without further purification unless otherwise mentioned. Ethyl (dimethylaminopropyl) carbodiimide (EDC) and *N*-hydroxysuccinimide (NHS) were purchased from JenKem Technology USA, Inc. (Allen, TX, USA). Dialysis membrane (cutoff = 7 kDa MWCO). *N*-Isopropyl acrylamide (NIPAM), cysteamino hydrochloride, 3-aminopropyl-trimethoxysilan (APTS), ammonium persulfate, *N*,*N*,*N*′,*N*′-tetramethylethylenediamine (TMED), and gelatin were purchased from ACROS (New Jersey, USA). SWNTs were purchased from US Research Nanomaterials. Photo-dynamic therapy 630 Type II (976 nm wavelength) Laser Tumor Therapeutic Apparatus (Xingda, China) was employed as a near-infrared irradiation apparatus.

Methodology—Preparation of Oxidized SWNTs: The oxidized SWNTs were prepared based on a previous research.[14] Briefly, the solution contained 98% H_2SO_4 and 65% HNO_3 with volume ratio of 3 to 1 was first prepared. 50 mg of SWNTs was then added to the solution, the mixture was then sonicated for 24 h at 0 °C. Ultrapure water (18.2 MΩ) was then utilized to rinse the oxidized SWNTS for five times. The mixture was next centrifuged with the speed of 13 000 rpm for three times with each time for 10 min. The oxidized SWNTs were collected from deposit and the black powder was gained by lyophilization.

Preparation of SWNT-APTS: 100 mg of treated SWNTs was added to the solution of 10 g 3-aminopropyl-trimethoxysilan, 100 mL ethanol (95%), and 1 mL acetic acid (99.7%). Then, the mixture was ultrasonic for 10 min following by 30 min centrifuge. The centrifuge was repeated for three times with the speed of 12 000 rpm, each round was last 10 min and the composite was rinsed with DD water for three times. The black powder of SWNT-APTS collected from deposit was obtained by lyophilization. The preparation of SWNT-APTS was determined by FTIR test. Fourier transform infrared spectroscopy (FTIR) test was adopted applying an IR Spectrophotometer (Bruker IFS 66v/s, German) within limits between 4000 and 400 cm^{-1}.

Preparation of Gelatin/SWNT-APTS: 1 g gelatin was resolved in 100 mL trifluoroethanol (TFE) for 24 h. 60 mg black powder of SWNT-APTS was then added to 100 mL gelatin solution (1%) following by 30 min ultrasonic. The solution was then stirred for 24 h. The solution was then centrifuged for 1 h. The centrifuge was repeated for three times with the speed of 12 000 rpm, each round lasted 20 min and the composite was washed by DD water for three times, and the deposit was collected. gelatin/SWNT-APTS was collected after dried in high vacuum for 24 h. The preparation of gelatin/SWNT-APTS was determined by FTIR test.

Synthesis of pNIPAM-NH_2 Composite: The mixture of 550 mg NIPAM, 25 mg cysteamine, 100 µL APS, and 6 mL Milli-Q water was heated to 70 °C for 3 h in N_2 atmosphere. The solution was then dialyzed against Milli-Q water for 2 d. The PNIPAM-NH2 polymer was collected through lyophilization. The synthesis of PNIPAM-NH2 polymer was determined by FTIR test.

Preparation of Gelatin/SWNT-APTS-NH_2: The 10 mg gelatin/SWNT-APTS composite was precipitation dispersed in the solution consisting of 10 mL 7.4 PBS buffer (0.1 M), 120 mg EDC, and 70 mg NHS. Finally, 154 mg PNIPAM-NH_2 was added to the solution for crosslinking. After dialysis (with cutoff MW: 1000 D) against PBS buffer for 4 d, the final product was obtained by lyophilization with carbon nanotube around 6%. The characterization of gelatin/SWNT-APTS-NH_2 was determined by FTIR test.

TEM Study on SWNT-GEL: The SWNT-GEL powder was dissolved in deionized water on ice to obtain a final concentration of 20 mg mL^{-1} and stored at 4 °C. 2 µL droplet-sized SWNT-GEL solution was fixed onto a TEM-specialized copper grid for sample preparation. No extra staining was added. Microstructure and general feature of SWNT-GEL were obtained and photographed using a Hitachi TEM system operating at 80 kV. Images were captured at 10 000× to 40 000× magnification.

Drug Release of DOX/SWNT-GEL in PBS: Powder of DOX was dissolved in PBS (pH 7.4) to obtain DOX solution at a concentration of 1.25 µg $µL^{-1}$. While SWNT-GEL was also dissolved in PBS to acquire homogeneous suspension of 30 mg mL^{-1} concentration. In each sample, 100 µg DOX solution was added to 300 µL SWNT-hydrogel suspension with vigorous mix and vortex. The DOX/SWNT-GEL was transferred into 1.5 mL EP tube in triplicate and kept in thermostatic incubator at 43 °C during the whole course of experiment. After 24 h incubation, gelatin was formed stably; 1 mL preheated fresh PBS was added on the surface of each hydrogel sample. Afterward, 100 µL supernatant was displaced with 100 µL fresh PBS after taken out for drug release test at predefined time intervals for 28 d. The DOX released from DOX/SWNT-GEL was measured through optical density (OD) absorbance at 480 nm (SpectraMax M5, Molecular Devices, USA).

Cellular Uptake Assay: BGC-823 gastric cancer cell line was cultured with RPMI1640 added with 10% fetal bovine serum (FBS), 1.0×10^5 U L^{-1} penicillin, and 100 mg L^{-1} streptomycin at 37 °C in 5% CO_2. After primary incubation, BGC cells were collected and seeded in a six-well tissue culture plate with culture density of 2×10^5 cells per well. Fresh culture medium and DOX/SWNT-GEL commixture was added at different time intervals after cells attached to the culture surface of each well. The cellular uptake rate was observed using a fluorescent microscopy after 0.5, 2, and 24 h incubation.

Cell Viability Assay: The cytotoxicity of the released cells incubated with DOX and SWNT-GEL with or without laser treatment was investigated applying a methylthiazoltetrazolium bromide (MTT) assay. BGC-823 cells were cultured as afore-mentioned and seeded in a 96-well tissue culture plate with culture density of 5000 cells per well. After 24 h, the growth medium was removed and fresh RPMI1640 were added. Then, the DOX and SWNT-GEL were added to each well separately; the wells added with SWNT-GEL were irradiated with 976 nm laser for 0 s, 15 s, and 3 min. 20 µL MTT solutions were added after 24 h incubation, and the cells were incubated for another 4 h. 150 µL DMSO were next added to wells to dissolve formazan. ELISA plate reader was then applied to examine the absorbance of each well at wavelength of 570 nm. The cell viability was then calculated as the following formula:

$$\text{Cell viability rate} = OD_{treat}/OD_{control} \times 100\% \quad (1)$$

where OD_{treat} and $OD_{control}$ are the optical density (OD) explored for cells treated with different treatments and for control cells (untreated), respectively.

Flow Cytometry Measurement: To assess the apoptosis and cell death ratio, flow cytometry experiment was carried out. First, the DOX/SWNT-GEL was prepared by physically mixed DOX with SWNT-GEL to obtain stabilized and homogeneous suspension, the mixed solution was vortexed and centrifuged till homogenized. Cells were incubated in six-well culture plate and given three different treatments: PBS blank control, free DOX, and DOX/SWNT-GEL (NIR

© 2015 WILEY-VCH Verlag GmbH & Co. KGaA, Weinheim

irradiated) groups. After 6 h incubation, cells were collected and dyed with Annexin V-FITC/PI Apoptosis Detection Kit and taken for FCM detect immediately.

In Vivo Experiment of DOX-Loaded SWNT Hydrogel Hybrid: Gastric cancer cell line BGC-823 was cultured with RPMI1640 (Hyclone) added with 10% FBS and incubated at 37 °C in 5%CO_2 in a humidified atmosphere. Cells were trypsinized and suspended with PBS when reached a confluence of 80%. 24 BALB/c nude mice (male, 4 weeks old) were purchased from the Laboratory Animal Center of Nanfang Hospital, Southern Medical University. Experiments on animals were complied with the protocols of the animal center. Each mouse was fed for 1 week's acclimation before injected with 2.5×10^6 BGC cells in 150 µL PBS into subcutaneous tissue of the left dorsal to establish xenograft gastric tumor model. When the tumor volume reached about 100 mm^3, mice were randomized to four groups treated with: 1) PBS, 2) free DOX, 3) SWNT-GEL alone, 4) DOX/SWNT-GEL, respectively. Besides, three mice in each group were assigned randomly to receive NIR radiation at the tumor site 1 d after the treatments with the photodynamic apparatus (976 nm, 200 mW cm^{-2}, 10 min). In the aforementioned treatments, DOX was given at a dose of 2 mg kg^{-1} and SWNT hydrogel at a concentration of 20 mg mL^{-1}. All of the treatments were administrated intratumorly. Tumor volumes were measured every 3 d for a consecutive 4 weeks and calculated as the formula: V_T = length × width^2/2. The body weight of each mouse was recorded once a week.

Hematoxylin Eosin (HE) Staining and Fluorescence Detection: All mice were sacrificed on the 28th day after treatment. Tumor tissues and four main organs (heart, liver, kidney, and spleen) were harvested, fixed with 4% paraformaldehyde, and paraffin embedded for HE staining. Meanwhile, tumors treated with DOX and DOX/SWNT-GEL were collected and placed in liquid nitrogen for frozen section; tissue sections were obtained for DAPI staining following with fluorescent microscopic detection.

Micro-Positron Emission Tomography-Computed Tomography (Micro PET-CT) Detection: The in vivo detection of tumor glucose metabolism activity was carried out with micro PET-CT. ^{18}F-2-deoxy-2-fluoro-D-glucose (^{18}F-FDG) was used as the radiotracer. One mouse in each group was taken for PET-CT scan. All mice were anesthetized with 1% pentobarbital (6 mL kg^{-1}) intraperitoneally and then injected with ^{18}F-FDG (10 mCi kg^{-1}) through the tail vein 1 h before the scan. The scan was performed on the day before treatment, 15 d and 28 d after treatment.

Statistical Analysis: The repeated measures general linear model was employed to analyze differences between groups of mice tumor volumes. Data are presented as mean values ± SD of multiple determinations. *P* values of <0.05 were considered statistically significant, and all statistical calculations were done with IBM SPSS 20.0.

Supporting Information

Supporting Information is available from the Wiley Online Library or from the author.

Acknowledgements

Z.M. and L.S. contributed equally to this work. This work was supported by the NSERC Discovery Grant (M.M.Q.X. and W.Z.) and NSERC RTI Grant, and Manitoba Children's Foundation. Acknowledgement also comes to Dr. Malcolm Xing, Dr. Wen Zhong, all the colleagues, and Manitoba Institute of Child Health.

Received: April 9, 2015
Revised: May 16, 2015
Published online: June 26, 2015

[1] a) A. Jemal, F. Bray, M. M. Center, J. Ferlay, E. Ward, D. Forman, *CA Cancer J. Clin.* **2011**, *61*, 69; b) S. R. Alberts, *Ann. Oncol.* **2003**, *14*, 31ii; c) D. M. Parkin, J. Ferlay, M. P. Curado, F. Bray, B. Edwards, H. R. Shin, D. Forman, *Int. J. Cancer* **2010**, *127*, 2918.

[2] a) Y. Octavia, C. G. Tocchetti, K. L. Gabrielson, S. Janssens, H. J. Crijns, A. L. Moens, *J. Mol. Cellular Cardiol.* **2012**, *52*, 1213; b) Z. Heger, N. Cernei, J. Kudr, J. Gumulec, I. Blazkova, O. Zitka, T. Eckschlager, M. Stiborova, V. Adam, R. Kizek, *Int. J. Mol. Sci.* **2013**, *14*, 21629.

[3] a) A. Bilici, *World J. Gastroenterol.* **2014**, *20*, 3905; b) E. U. Cidon, S. G. Ellis, Y. Inam, S. Adeleke, S. Zarif, T. Geldart, *Cancers* **2013**, *5*, 64; c) M. Rybinski, Z. Szymanska, S. Lasota, A. Gambin, *J. R. Soc. Interface* **2013**, *10*, 20130527.

[4] a) C. H. Chung, *Oncologist* **2008**, *13*, 725; b) G. Calogiuri, M. T. Ventura, L. Mason, A. Valacca, R. Buquicchio, N. Cassano, G. A. Vena, *Curr. Pharm. Des.* **2008**, *14*, 2883; c) D. E. Ferastraoaru, M. N. Dickler, S. Patel, E. A. Fischer, M. P. Pulitzer, P. L. Myskowski, E. Jerschow, *J. Clin. Oncol.* **2013**, *31*, e407; d) J. Giuliani, *Med. Oncol.* **2012**, *29*, 3597.

[5] G. S. Thakor, S. S. Gambhir, *CA Cancer J. Clin.* **2013**, *63*, 395.

[6] a) R. Weissleder, *Nat. Biotechnol.* **2001**, *19*, 316; b) C. R. Simpson, M. Kohl, M. Essenpreis, M. Cope, *Phys. Med. Biol.* **1998**, *43*, 2465; c) S. Liu, A. Ko, W. Li, W. Zhong, M. Xing, *J. Mater. Chem. B* **2014**, *2*, 1125.

[7] V. Ntziachristos, J. Ripoll, L. H. V. Wang, R. Weissleder, *Nat. Biotechnol.* **2005**, *23*, 313.

[8] a) P. Huang, C. Zhang, C. Xu, L. Bao, Z. Li, *Nano Biomed. Eng.* **2010**, 225; b) B. Kang, D. Yu, Y. Dai, S. Chang, D. Chen, Y. Ding, *Small* **2009**, *5*, 1292; c) N. W. S. Kam, H. J. Dai, *J. Am. Chem. Soc.* **2005**, *127*, 6021; d) D. Pantarotto, R. Singh, D. McCarthy, M. Erhardt, J. P. Briand, M. Prato, K. Kostarelos, A. Bianco, *Angew. Chem. Int. Ed.* **2004**, *43*, 5242; e) K. Kostarelos, L. Lacerda, G. Pastorin, W. Wu, S. Wieckowski, J. Luangsivilay, S. Godefroy, D. Pantarotto, J.-P. Briand, S. Muller, M. Prato, A. Bianco, *Nat. Nanotechnol.* **2007**, *2*, 108; f) Y. L. iu, D. Wu, W. Zhang, X. Jiang, C. He, T. Chung, S. Goh, K. Leong , *Angew. Chem. Int. Ed.* **2005**, *44*, 4782; g) N. Kam, L. Zhuang, H. Dai, *Am. Chem. Soc.* **2005**, *127*, 12492.

[9] a) M. Foldvari, M. Bagonluri, *Nanomed.-Nanotechnol. Biol. Med.* **2008**, *4*, 183; b) Z. Liu, S. Tabakman, K. Welsher, H. Dai, *Nano Res.* **2009**, *2*, 85.

[10] a) G. Pastorin, W. Wu, S. Wieckowski, J. P. Briand, K. Kostarelos, M. Prato, A. Bianco, *Chem. Commun.* **2006**, *11*, 1182; b) Z. Liu, X. Sun, N. Nakayama-Ratchford, H. Dai, *ACS Nano* **2007**, *1*, 50.

[11] a) E. Ruel-Gariépy, J.-C. Leroux, *Eur. J. Pharm. Biopharm.* **2004**, *58*, 409; b) J. Chen, X. Qiu, L. Wang, W. Zhong, J. Kong, M. M. Q. Xing, *Adv. Funct. Mater.* **2014**, *24*, 2216.

[12] a) Y. Guan, Y. Zhang, *Soft Matter* **2011**, *7*, 6375; b) J. Shi, W. Guobao, H. Chen, W. Zhong, X. Qiu, M. M. Q. Xing, *Polym. Chem.* **2014**, *5*, 6180.

[13] W. S. Muhammad, I. Tzannou, N. Makrilia, K. Syrigos, *Yale J. Biol. Med.* **2010**, *83*, 53.

[14] J. Ren, S. Shen, D. Wang, Z. Xi, L. Guo, Z. Pang, Y. Qian, X. Sun, X. Jiang, *Biomaterials* **2012**, *33*, 3324.

© 2015 WILEY-VCH Verlag GmbH & Co. KGaA, Weinheim